A ripple suppression strategy based on virtual self-injection APF for quasi-Z source inverter

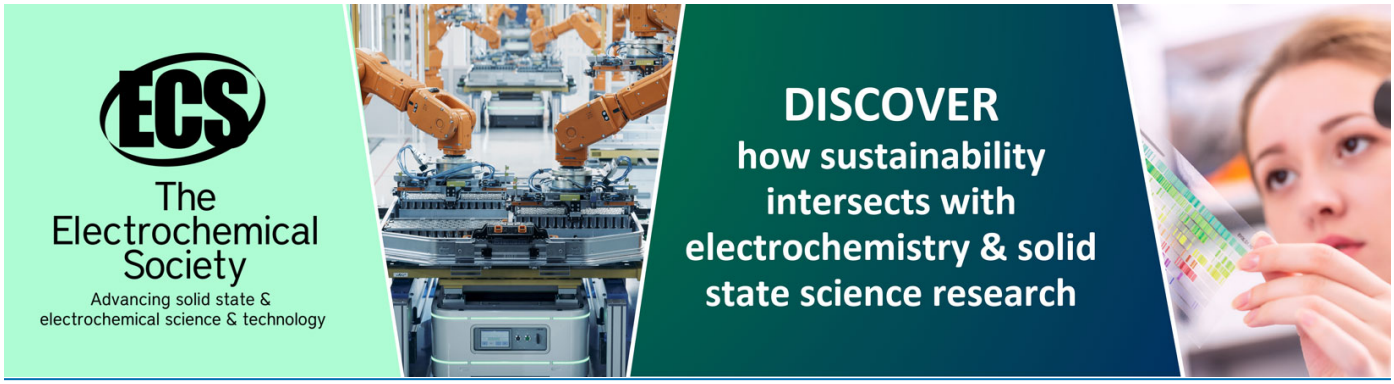

A ripple suppression strategy based on virtual self-injection APF for quasi-Z source inverter

R Y Wei[1], Y F Tang[1], S J Wang[2] and Z Y Li[1,3]

[1]School of Information Science and Engineering, Central South University, Changsha 410083, Hunan Province, China
[2]Design and Research Institute CO. LTD. of CREEC, Kunming, 650200, Yunnan Province, China

Email: lizy@csu.edu.cn

Abstract. The power flows between the DC side and AC side of single-phase quasi-Z source inverter (QZSI) causes double-frequency (2ω) voltage ripple of capacitors, current ripple of inductors. This paper proposes a virtual self-injection active power filter (APF) ripple suppression strategy for the single-phase QZSI without changing the circuit structure, and the 2ω ripple is suppressed by controlling the shoot-through duty cycle based on the thought of ripple vector cancellation. The 2ω ripple model and its generation mechanic for single-phase QZSI are presented through the analysis of the power flows and small signal model for quasi-Z network. Simulation results verify the proposed ripple suppression strategy can effectively reduce the 2ω current ripple of inductors from 18.38% to 3.54%.

1. Introduction

The QZSI has recently attracted much attention in the grid-connected photovoltaic systems because of its higher booster, no dead-time compare to traditional inverter, and its less active switches, lower cost, almost the same or higher efficiency compared to the two-stage inverter [1-6]. The 2ω power flows between the DC side and AC side of QZSI causes 2ω voltage ripple of capacitors, current ripple of inductors [3,4]. It also will lead to the DC source to produce a 2ω ripple component in its output current. When the ripple component flows into passive devices, it will cause the temperature increasing of passive devices, which seriously affects their working life.

Due to the 2ω ripple will bring a lot of harms to the grid-connected photovoltaic systems and quasi-Z network, it is necessary to minimize or restricted them to an engineering tolerant range. The traditional method of ripple suppression is to research the capacitance and inductance of quasi-Z network [5,6]. But this method will not only lead to high volume, high weight and high cost, but also reduce reliability and efficiency due to the use of large capacity capacitors and inductance inductors. In [3], a new modified modulation and an input ripple controller are used to prevent the ripple energy flowing into the DC side instead of using large capacitance. In [7], a low frequency voltage was added to the constant voltage for generating the variable shoot-through time intervals, and this method can improve the AC output quality of the inverter. In [8], a discrete-time average model-based predictive control is proposed, this method is used to reduce voltage and current ripple by predicting future behaviors of the shoot-through duty cycle and modulation signals.

The APF technology is another ripple suppression strategy. In [4] and [9], the APF consists of extra switches, capacitors and inductors, it will inject reverse current into the circuit by control of switch

and can effectively reduce the ripple, but extra circuit means higher cost. In [10], two space vector modulation strategies was proposed, which control the distribution of shoot-through duty cycle in the switch period to reduce the inductor current ripple. In [11], a ripple suppression strategy based on feedback control has been proposed, which is designed to generate a small variation shoot-through duty cycle to reduce the 2ω ripple of the inductor current by extracting the actual DC side inductor current ripple.

This paper proposes a virtual self-injection APF ripple suppression strategy to reduce the 2ω current ripple of inductors without changing the circuit structure of QZSI. By controlling the variation of shoot-through duty cycle and utilizing the filtering effect of quasi-Z network to suppress the 2ω ripple. This paper organized as follows. Section 2 focuses on the circuit analysis, operation principle, and deriving the 2ω ripple model for single-phase QZSI. Section 3 discusses the mechanism of 2ω ripple production. Section 4 presents the virtual self-injection APF ripple suppression strategy. Finally, simulation results are provided to verify the effectiveness of the proposed strategy.

2. Circuit analysis of single-phase QZSI

The single-phase QZSI includes the H-bridge and the quasi-Z network two parts, as shown in figure 1. The quasi-Z network consists of the inductors L_1, L_2, the capacitors C_1, C_2 and a diode. Compared to traditional inverters, the QZSI can increase voltage gain and avoid dead time in conjunction with planned shoot-through states.

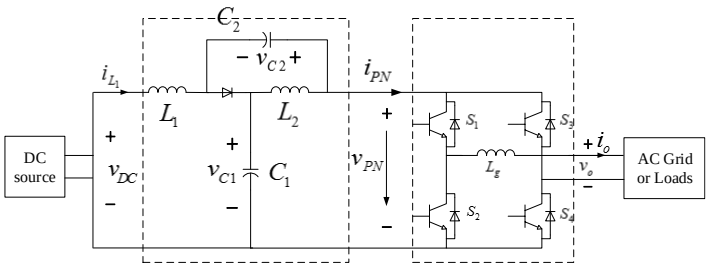

Figure 1. Single-phase QZSI.

The operating states of the QZSI can be simplified into shoot-through state and non-shoot-through state. The equivalent circuit of shoot-through state is shown in the figure 2(a), the diode is cut off and both of the power switches in a leg of the H-bridge are turned on at the same time. Thus, in this state, the DC-link voltage v_{PN} is zero and the inverter does not generate power to AC grid or loads. In the non-shoot-through state, as shown in figure 2(b), the diode turns on and the inductors charge the capacitors, the inverter outputs power.

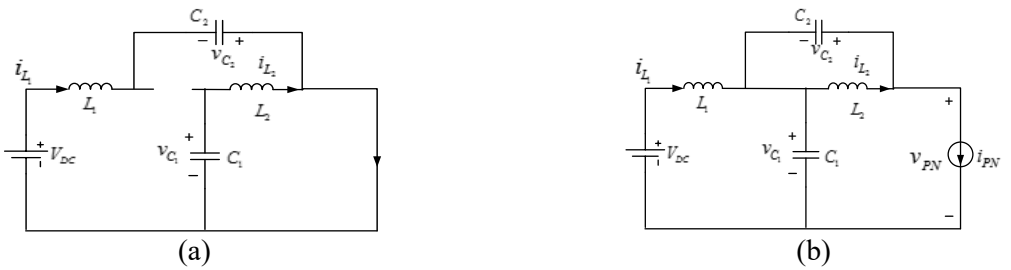

Figure 2. Equivalent circuits of single-phase QZSI in shoot-through state (a) and non-shoot-through state (b).

From figure 2, using state-space average method, the state space averaged model of quasi-Z network is derived by

$$\begin{cases} L_1 \dfrac{di_{L_1}}{dt} = V_{DC} - (1-d)v_{C_1} + dv_{C_2} \\ L_2 \dfrac{di_{L_2}}{dt} = -(1-d)v_{C_2} + dv_{C_1} \\ C_1 \dfrac{d\upsilon_{C_1}}{dt} = (1-d)(i_{L_1} - i_{PN}) - di_{L_2} \\ C_2 \dfrac{d\upsilon_{C_2}}{dt} = (1-d)(i_{L_2} - i_{PN}) - di_{L_1} \end{cases} \tag{1}$$

where d is the shoot-through duty cycle, and d , i_{L_1} , i_{L_2} , v_{C_1} , v_{C_2} can be expressed as

$$d = D + \hat{d} \text{ , } i_{L_1} = I_{L_1} + \hat{i}_{L_1} \text{ , } i_{L_2} = I_{L_2} + \hat{i}_{L_2} \text{ , } v_{C_1} = V_{C_1} + \hat{v}_{C_1} \text{ , } v_{C_2} = V_{C_2} + \hat{v}_{C_2} \tag{2}$$

where D is the average shoot-through duty cycle, I_{L_1} and I_{L_2} are the average value of inductor current, V_{C_1} and V_{C_2} are the average value of capacitor voltage, $\hat{d}$, $\hat{i}_{L_1}$, $\hat{i}_{L_2}$, $\hat{v}_{C_1}$, $\hat{v}_{C_2}$ are their variations respectively.

From equation (2) and using the small signal analysis method for equation (1), we can obtain the dynamic small-signal model as

$$\begin{cases} L_1 \dfrac{d\hat{i}_{L_1}}{dt} = -(1-D)\hat{v}_{C_1} + D\hat{v}_{C_2} + (\mathrm{V}_{C_1} + \mathrm{V}_{C_2})\hat{d} \\ L_2 \dfrac{d\hat{i}_{L_2}}{dt} = -(1-D)\hat{v}_{C_2} + D\hat{v}_{C_1} + (\mathrm{V}_{C_1} + \mathrm{V}_{C_2})\hat{d} \\ C_1 \dfrac{d\hat{\upsilon}_{C_1}}{dt} = (1-D)\hat{i}_{L_1} - D\hat{i}_{L_2} - (1-D)\hat{i}_{PN} + (I_{PN} - I_{L_1} - I_{L_2})\hat{d} \\ C_2 \dfrac{d\hat{\upsilon}_{C_2}}{dt} = (1-D)\hat{i}_{L_2} - D\hat{i}_{L_1} - (1-D)\hat{i}_{PN} + (I_{PN} - I_{L_1} - I_{L_2})\hat{d} \end{cases} \tag{3}$$

In order to simplify the calculation and analysis, assuming that $L_1 = L_2 = L$, $C_1 = C_2 = C$. The small-signal model of quasi-Z network can be simplified as

$$\begin{cases} L \dfrac{d\hat{i}_L}{dt} = -(1-2D)\hat{v}_C + (V_{C_1} + V_{C_2})\hat{d} \\ C \dfrac{d\hat{v}_C}{dt} = (1-2D)\hat{i}_L - (1-D)\hat{i}_{PN} + (I_{PN} - 2I_{L_1})\hat{d} \end{cases} \tag{4}$$

Basing on the simplified small-signal model (4) and using the Laplace transform, we can obtain the ripple model of inductor current and capacitor voltage for the single-phase QZSI, as shown in equations (5) and (6), respectively.

$$\hat{i}_{L_1}(s) = \hat{i}_{L_2}(s) = \frac{(1-2D)(1-D)}{LCs^2 + (1-2D)^2}\hat{i}_{PN}(s) + \frac{CsV_{PN} - (1-2D)(I_{PN} - 2I_{L_1})}{LCs^2 + (1-2D)^2}\hat{d}(s) \tag{5}$$

$$\hat{v}_{C_1}(s) = \hat{v}_{C_2}(s) = \frac{-(1-D)Ls}{LCs^2 + (1-2D)^2}\hat{i}_{PN}(s) + \frac{(1-2D)V_{PN} + Ls(I_{PN} - 2I_{L_1})}{LCs^2 + (1-2D)^2}\hat{d}(s) \tag{6}$$

thus, the transfer function can be obtained as equations (7) and (8).

$$G_{\hat{i}_{PN}}^{\hat{i}_L}(s) = \frac{(1-D)(1-2D)}{LCs^2 + (1-2D)^2} \tag{7}$$

$$G_{\hat{d}}^{\hat{i}_L}(s) = \frac{(V_{C_1} + V_{C_2})Cs + I_{PN}}{LCs^2 + (1-2D)^2} \tag{8}$$

where equations (7) and (8) are the transfer function from $\hat{i}_{PN}$ to the $\hat{i}_L$ and the transfer function from $\hat{d}$ to $\hat{i}_L$, respectively.

3. Mechanism of ripple production

As shown in figure 1, the DC-link voltage and current of H-bridge are respectively expressed as

$$v_{PN} = V_{PN} + \hat{v}_{PN} \tag{9}$$

$$i_{PN} = I_{PN} + \hat{i}_{PN} \tag{10}$$

where V_{PN} is the average value of DC-link voltage, I_{PN} is the average value of DC-link current, $\hat{v}_{PN}$ is the voltage ripple, $\hat{i}_{PN}$ is the current ripple, respectively.

The input power of H-bridge can be expressed by

$$P_{PN} = (1-D)v_{PN}i_{PN} = (1-D)(V_{PN}I_{PN} + V_{PN}\hat{i}_{PN} + I_{PN}\hat{v}_{PN} + \hat{i}_{PN}\hat{v}_{PN}) \tag{11}$$

The amplitude of the AC output voltage and current for the QZSI can be defined as V_o and I_o, respectively. Thus, the AC output voltage v_o and output current i_o can be expressed as

$$v_o = V_o \sin(\omega t) \tag{12}$$

$$i_o = I_o \sin(\omega t - \varphi) \tag{13}$$

Therefore, the output power of inverter is

$$P_o = \frac{1}{2}V_o I_o \cos\varphi - \frac{1}{2}V_o I_o \cos(2\omega t - \varphi) \tag{14}$$

where ω is the fundamental angular frequency, φ is the impedance angle.

According to the conservation of energy theorem, we know the power generated by DC side in the non-shoot-through state is equal to the output power because the DC-link voltage is zero and no power is generated in the shoot-through state.

$$P_{PN} = P_o \tag{15}$$

The voltage ripple $\hat{v}_{PN}$ and current ripple $\hat{i}_{PN}$ is much small to ignore $\hat{v}_{PN} \times \hat{i}_{PN}$. At the same time, we usually ignore $\hat{v}_{PN}$, and from (11), (14) and (15), the DC-link current i_{PN} can be calculated by

$$i_{PN}(t) = \frac{MI_o}{2(1-D)}\left[\cos\varphi - \cos\left(2\omega t - \varphi\right)\right] \tag{16}$$

where M is the modulation index of inverter.

From equation (16), the current i_{PN} consist of the DC component and the 2ω ripple component, and $\hat{i}_{PN}$ is

$$\hat{i}_{PN}(t) = \frac{MI_o}{2(1-D)}\left[\cos(2\omega t - \varphi)\right] \tag{17}$$

From equations (7) and (17), there is 2ω power flows between the AC side and DC side of inverter, and this 2ω power will cause 2ω inductor current ripple.

4. Virtual self-injection APF ripple control strategy

4.1. Control strategy

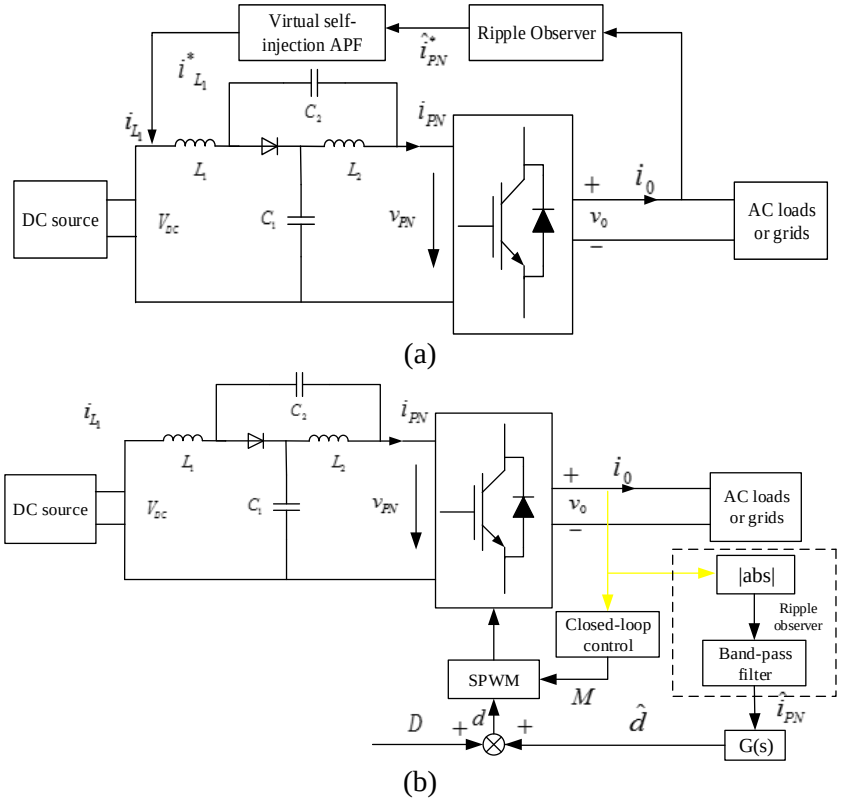

Figure 3. Block diagram of proposed virtual self-injection APF ripple suppression strategy.

From (5) and (6), the changes of $\hat{i}_L$ and $\hat{v}_C$ relate to variations $\hat{i}_{PN}$ and $\hat{d}$. From transfer functions (7) and (8), if the shoot-through duty cycle has a variation $\hat{d}$, the DC-link current will contain a variation $\hat{i}_{PN}^*$. Therefore, regarding $\hat{i}_{PN}$ as a disturbance and $\hat{i}_{PN}^*$ can be seen as the compensation current, which is generated by H-bridge using the compensation control signal $\hat{d}$. When $\hat{i}_{PN}^*$ flows into the quasi-Z network, the compensation current $\hat{i}_{L_1}^*$ will be generated to offset the inductor current ripple $\hat{i}_{L_1}$, this method is called ripple vector cancellation. The control block diagram is shown in figure 3, the compensation control signal of the shoot-through duty cycle $\hat{d}$, together with SPWM control and the quasi-Z network make up the virtual self-injection APF. The ripple observer consists of the absolute

value processing and band-pass filter, and the compensation current $\hat{i}_{L_1}^*$ is the output of the proposed control system. Finally, the proposed virtual self-injection APF ripple suppression strategy is formed to suppress the 2ω inductor current ripple with the quasi-Z network by controlling the shoot-through duty cycle.

For traditional QZSI, the shoot-through duty cycle D can provide a certain voltage boost character. Compared with the traditional QZSI control strategy, the shoot-though duty cycle control signal is no longer a constant signal and the actual shoot-through duty cycle d with the proposed ripple suppression strategy is

$$d = D + \hat{d} \tag{18}$$

The shoot-through duty cycle compensation control signal is expressed by

$$\hat{d}(s) = -\hat{i}_{PN}(s)\frac{G_{\hat{i}_{PN}}^{\hat{i}_L}(s)}{G_{\hat{d}}^{\hat{i}_L}(s)} = -\hat{i}_{PN}G(s) \tag{19}$$

From (7), (8) and (19), the transfer function of the ripple suppressor is

$$G(s) = \frac{(1-D)(1-2D)}{C(V_{C_1} + V_{C_2})s + I_{PN}} \tag{20}$$

4.2. Ripple observer

The premise of proposed ripple suppression strategy is how to accurately acquire the 2ω component. But the DC-link current i_{PN} is hard to sample due to the existence of shoot-through state, and the waveform of i_{PN} is shown in figure 4. Therefore, in order to ensure the control accuracy, the system design to use a soft sensing technology that sampling the AC output current i_o by a band-pass filter instead of i_{PN} .

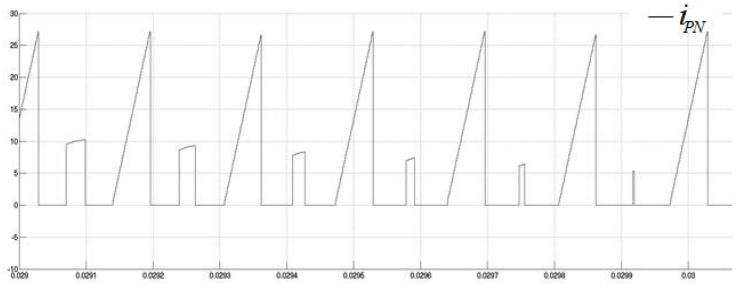

Figure 4. The waveform of DC-link current i_{PN} .

After sampling the current $\hat{i}_o$, on the one hand, the H-bridge modulation signal is generated by the output closed loop control of the H-bridge, on the other hand, the disturbance $\hat{i}_{PN}$ is obtained by calculating the $\hat{i}_o$. We can get a disturbance compensation signal $\hat{d}$ after processing the $\hat{i}_{PN}$ by the ripple suppression controller. Due to the current i_o and i_{PN} are not synchronized and in order to get the $\hat{i}_{PN}$ better, we need to take the absolute value of i_o. From (13), the Fourier series expansion of $|i_o|$

can be given by

$$\left|i_o(t)\right| = I_o\left|\sin(\omega t-\varphi)\right| = \frac{2I_o}{\pi} + \frac{4I_o}{\pi}\sum_{n=1}^{\infty}\frac{\cos(2n\omega t-\varphi)}{1-4n^2} \tag{21}$$

The band-pass filter is used to minimize the influence of the non-2ω components. Due to the resonant frequency of the filter is 100Hz, $n=1$ can be calculated, and from (17) and (21), the resonance gain of band-pass filter K is

$$K = \frac{MI_o}{2(1-D)} \div \frac{4I_o}{3\pi} = \frac{3\pi M}{8(1-D)} \tag{22}$$

5. Simulation analysis

In order to verify the proposed ripple suppression strategy, a simulation circuit model of QZSI is built by using SIMULINK in this paper. The parameters of simulation model are listed in table 1.

Table 1. Parameters of the simulation model.

Parameters	Value
Quasi-Z network capacitor C_1, C_2 (mF)	1.5
Quasi-Z network inductor L_1, L_2 (mH)	1
Filter inductor L_g (mH)	4
Input DC source v_{DC} (V)	85
Switching frequency (kHz)	3×10^3
Shoot-through duty cycle D	1/3
Modulation ratio M	0.6

The main emphasis of the proposed strategy is the analysis and acquisition of disturbance compensation shoot-through duty cycle $\hat{d}$. Figure 5 shows two different control signal waveforms of shoot-through cycle duty, where the red curve shows the waveform of the control signal for D, it is a linear and its value is a constant. The sum of D and $\hat{d}$ is the actual shoot-through duty cycle's control signal d for the proposed ripple suppression strategy, as shown in blue curve.

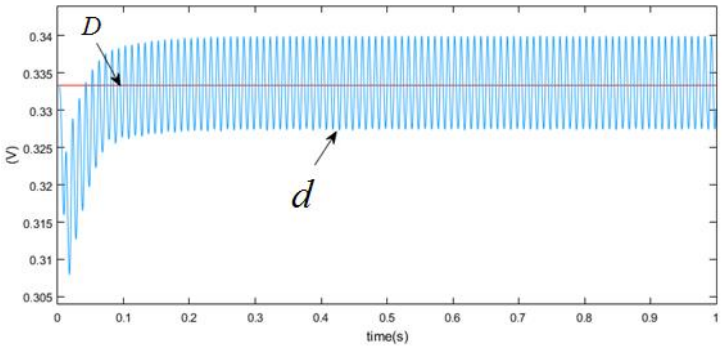

Figure 5. The control signal waveforms of shoot-through duty cycle.

Figure 6 shows the simulation waveforms of i_{L_1} without and with the proposed suppression

strategy. And from figure 6(a), i_{L_1} contains ripple components with large amplitude and high ratio. However, current ripples are significantly reduced when the strategy is applied, as shown in figure 6(b).

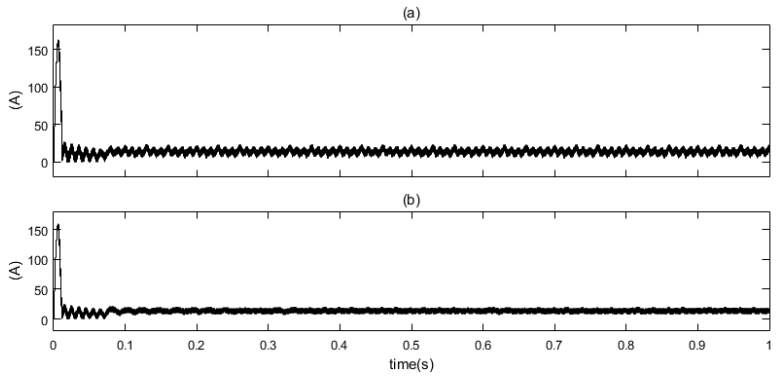

Figure 6. Simulation results of the current i_{L_1} without (a) and with (b) the ripple suppression strategy.

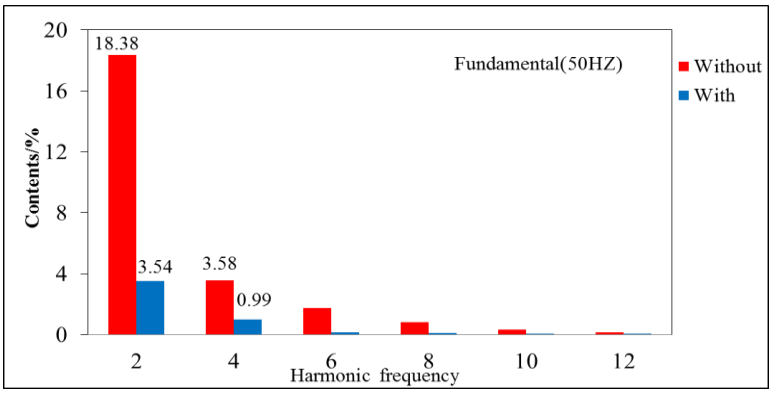

Figure 7. Simulation results for the content of ripples.

In order to further quantify the inhibitory effect of the proposed control strategy on ripple, the FFT decomposition of i_{L_1} (i_{DC}) is carried out, as shown in figure 7, and the red and blue bars show contents of harmonics without and with the control strategy, respectively. It can be seen that the current i_{DC} contains a large number of two, four, six and eight frequency harmonics when the ripple suppression strategy is not adopted, the content of 2ω current ripple was the highest and reaches 18.38%. The content of inductor 2ω current ripple has been significantly dampened to 3.54% with the proposed strategy. In addition, the other even harmonics, such as four, six frequency ripple also have also been dampened, and the contents of these have been reduced to less than 1%. The simulation results verify the proposed ripple suppression strategy can restrain ripples effectively, especially the 2ω inductor current ripple.

From the analysis above, we know the 2ω power ripple causes high ratios of 2ω ripple to inductor current, capacitor and dc-link voltages, which result in the distortion of inverter output current. Figure 8 shows the simulation waveforms of the output current of QZSI without (a) and with (b) the proposed strategy, and (c) shows the difference between (a) and (b). From figure 8(a) and (b), the output current is a relatively pure sinusoidal wave and not distorted, the deviation current is very small and fluctuates near zero, as shown in figure 8(c). The results show that the proposed ripple suppression strategy has no effect on the AC output current because it mainly uses the quasi-Z network to suppress the AC

component flows from the PN side to the DC source side.

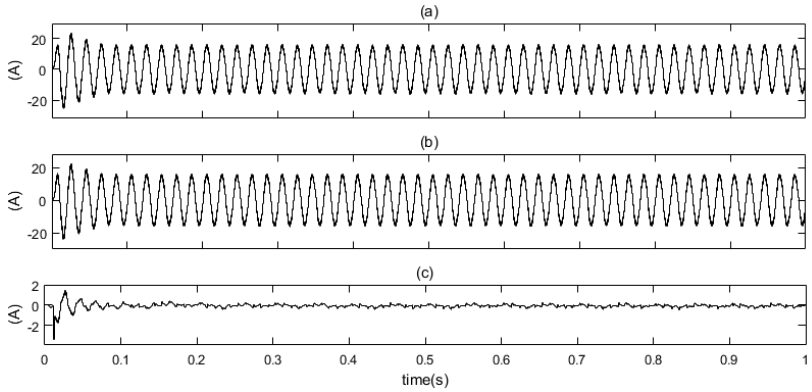

Figure 8. Simulation results of i_o without (a) and with (b) the ripple suppression strategy. (c) The difference between these two different states.

6. Conclusion

This paper proposed a virtual self-injection APF ripple suppression strategy to reduce DC side 2ω inductor current ripple without changing the structure and parameters of the circuit. The 2ω ripple model is derived through the analysis of power flows, the small-signal model and the transfer functions of quasi-Z network. Based on the ripple self-injection mechanism, it has been found the DC side 2ω inductor current ripple can be compensated by controlling the shoot-through duty cycle. Theoretical analysis and simulation results verified the proposed can effectively reduce the DC side 2ω current ripple of single-phase QZSI. The proposed strategy can improve the stability of QZSI at a relatively low cost. And the proposed strategy can be used in photovoltaic system and micro-grid system applications with its attractive features.

References

[1] Ayad A and Kennel R. 2017. A comparison of quasi-z-source inverters and conventional two-stage inverters for pv applications. *Epe Journal*. 27 43-59.

[2] Battiston A, Martin J P, Miliani E H and Nahid-Mobarakeh B. 2014 Comparison criteria for electric traction system using z-source/quasi z-source inverter and conventional architectures *IEEE J. Emerg. Sel. Topics Power Electron.* 2 467-76

[3] Zhou Y, Li H B and Li H. 2016. A single-phase pv quasi-z-source inverter with reduced capacitance using modified modulation and double-frequency ripple suppression control. *IEEE Trans. Power Electron.* 31 2166-73.

[4] Ge B, Liu Y, Abu-Rub H. et al. 2016. An active filter method to eliminate dc-side low-frequency power for a single-phase quasi-z-source inverter. *IEEE Trans. Ind. Electron.* 63 4838-48.

[5] Sun D, Ge B, Yan X, Abu-Rub H. et al. 2013. Impedance design of quasi-Z source network to limit double fundamental frequency voltage and current ripples in single-phase quasi-Z source inverter. *IEEE Energy Convers. Congr. Expo.* (Denver) 2745-50.

[6] Sun D, Ge B, Yan X and Bi D. 2014. Modeling, impedance design, and efficiency analysis of quasi-z source module in cascaded multilevel photovoltaic power system. *IEEE Trans. Ind. Electron.* 61 6108-17.

[7] Nguyen M K and Choi Y O. 2017. Maximum boost control method for single-phase quasi-switched-boost and quasi-z-source inverters. *Energies* 10 553.

[8] Liu Y, Abu-Rub H. et al. 2018. A Discrete-Time Average Model-Based Predictive Control for a Quasi-Z-Source Inverter. *IEEE Trans. Ind. Electron.* 65 6044-54.

[9] Singh S A, Azeez N A, Williamson S S. 2016. Capacitance reduction in a single phase Quasi Z-Source Inverter using a hysteresis current controlled active power filter. *IEEE International Symposium on Industrial Electronics* Santa Clara 6 805-10.
[10] He Y Y, Xu Y H and Chen J P. 2018. New space vector modulation strategies to reduce inductor current ripple of z-source inverters. *IEEE Trans. Power Electron.* 33 2643-54.
[11] Ge B, Liu Y, Abu-Rub H, et al. 2016. Current ripple damping control to minimize impedance network for single-phase quasi-z source inverter system. *IEEE Trans. Ind. Informat.* 12 1043-54.